

ISBN:

Advanced in Optics Photonics Spectroscopy & Applications XI

**Philippe Brechignac, Hyyong Suk, Nguyen Van Hieu,
N. Dai Hung, Valentin A. Orlovich, Nobuhiko Sarukura**



Publishing House for Science and Technology

CHẾ TẠO VÀ KHẢO SÁT ĐỂ SERS THANH NANO ZnO/Ag ỨNG DỤNG PHÁT HIỆN CHẤT HỮU CƠ ABAMECTIN Ở NỒNG ĐỘ THẤP.....	179
<i>Hoa Mai Anh, Nguyễn Hà Thanh, Đào Anh Tuấn, Nguyễn Hữu Kế, Lê Vũ Tuấn Hùng.....</i>	<i>179</i>
NGHIÊN CỨU KHẢ NĂNG HỖ TRỢ CHUYỂN ĐIỆN TÍCH CỦA MÀNG NHÔM MỎNG PHỦ TRÊN THANH ZnO NHẪM ỨNG DỤNG LÀM ĐẾ SERS.....	184
<i>Nguyễn Thành Phúc, Lê Thị Minh Huyền, Lê Vũ Tuấn Hùng.....</i>	<i>184</i>
TÍNH CHẤT DẪN ĐIỆN LOẠI p CỦA MÀNG SnO₂ ĐỒNG PHA TẠP n-Zn.....	190
<i>Đặng Hữu Phúc, Nguyễn Thị Mỹ Hạnh, Lê Thị Yến Nhung, Nguyễn Trần Hải Vân, Lê Trấn.....</i>	<i>190</i>
THE INFLUENCE OF THE SPUTTERING CURRENTS ON STRUCTURAL, OPTICAL AND ELECTRICAL PROPERTIES OF CuCr_{0.95}Mg_{0.05}O₂ THIN FILMS	195
<i>Dung Van Hoang, Tu Anh Kieu Le, Anh Tuan Thanh Pham, Truong Huu Nguyen, Ngoc Kim Pham, Hanh Kieu Thi Ta, Hanh Duc Thi Dinh, Dai Cao Truong, Hoa Thi Lai, Ngoc Van Le, Vinh Cao Tran, Thang Bach Phan.....</i>	<i>195</i>
ENHANCEMENT OF FLUORESCENT LABELING ALEXA VIA A SILVER THIN FILM	201
<i>Nguyen Thanh Thao, Nguyen Thuy An, Bach Thang Phan, Hanh Kieu Thi Ta, Thanh Van Thi Tran, Lai Thi Hoa, Kieu The Loan Trinh, and Nhu Hoa Thi Tran</i>	<i>201</i>
CHẾ TẠO VÀ KHẢO SÁT MỘT SỐ TÍNH CHẤT QUANG HỌC CỦA TINH THỂ KDP ĐỒNG PHA TẠP BRILLIANT GREEN VÀ EDTA.....	207
<i>Nguyễn Duy Nhật Nguyễn Văn Hạnh, Dư Quang Minh, Ngô Đức Lương, Phan Trung Vĩnh.....</i>	<i>207</i>
PHÁT HIỆN NỒNG ĐỘ THẤP CỦA THUỐC NHUỘM MÀU DỰA TRÊN ĐẾ SERS - DUNG DỊCH NANO Ag.....	212
<i>Tôn Nữ Quỳnh Trang, Nguyễn Duy Hải và Vũ Thị Hạnh Thu</i>	<i>212</i>
COMPARISON NONLINEARITY PROPERTIES OF LARGE AND SMALL SOLID CORE PHOTONIC FIBERS WITH As₂Se₃ SUBSTRATE	217
<i>Thuy Nguyen Thi, Duc Hoang Trong, Tran Tran Bao Le, Thanh Thai Doan, Vu Tran Quoc, Lanh Chu Van.....</i>	<i>217</i>
STUDY ON DISPERSION CHARACTERISTICS OF LARGE SOLID CORE PHOTONIC CRYSTAL FIBERS WITH As₂Se₃ SUBSTRATE.....	221
<i>Thuy Nguyen Thi, Duc Hoang Trong, Tran Tran Bao Le, Thanh Thai Doan, Vu Tran Quoc, Bao Le Xuan, Lanh Chu Van.....</i>	<i>221</i>
ẢNH HƯỞNG CỦA MỞ RỘNG DOPPLER LÊN SỰ LAN TRUYỀN XUNG LASER TRONG MÔI TRƯỜNG NGUYÊN TỬ BA MỨC CẤU HÌNH LAMBDA.....	225
<i>Lê Văn Đoài, Nguyễn Huy Bằng, Đinh Xuân Khoa, Đoàn Thanh Hoà, Trần Thị Xuân Thuý, Hoàng Minh Đông, Nguyễn Tuấn Anh và Lê Thị Minh Phương.....</i>	<i>225</i>

**THE INFLUENCE OF THE SPUTTERING CURRENTS
ON STRUCTURAL, OPTICAL AND ELECTRICAL PROPERTIES
OF $\text{CuCr}_{0.95}\text{Mg}_{0.05}\text{O}_2$ THIN FILMS**

**Dung Van Hoang^{1,2,3,*}, Tu Anh Kieu Le^{1,2,3}, Anh Tuan Thanh Pham^{1,2},
Truong Huu Nguyen^{1,2}, Ngoc Kim Pham^{2,3}, Hanh Kieu Thi Ta^{2,3},
Hanh Duc Thi Dinh^{1,2}, Dai Cao Truong^{2,5}, Hoa Thi Lai^{2,5},
Ngoc Van Le^{2,4}, Vinh Cao Tran^{1,2}, Thang Bach Phan^{1,2,5}**

¹*Laboratory of Advanced Materials, University of Science, HoChiMinh City, Vietnam*

²*Vietnam National University, HoChiMinh City, Vietnam*

²*Faculty of Materials Science and Technology, University of Science, Ho Chi Minh City, Vietnam*

⁴*Faculty of Physics and Engineering Physics, University of Science, Ho Chi Minh City, Vietnam*

⁵*Center for Innovative Materials and Architectures, HoChiMinh City, Vietnam*

Email: *hvdung@hcmus.edu.vn

Abstract. Magnesium-doped CuCrO_2 material has emerged as a p-type semiconductor because of its lowest resistivity in delafossite family. In this report, the $\text{CuCr}_{0.95}\text{Mg}_{0.05}\text{O}_2$ thin films were deposited on soda-lime glass substrate at the substrate temperature of 450°C from a 3-inch target of $\text{CuCr}_{0.95}\text{Mg}_{0.05}\text{O}_2$ material using dc magnetron sputtering system. From the XRD results, all films exhibit the significant existence of delafossite structure with the (110) orientation regardless sputtering currents and relatively low substrate temperature. There is a strong correlation between the structural and electrical properties of thin films as a function of the sputtering currents in which the higher integrated intensity of (110) orientation is, the lower the resistivity of the films is reached. The film deposited at current of 350 mA has the lowest resistivity of $4 \times 10^{-2} \Omega \cdot \text{cm}$.

Keywords: *$\text{CuCr}_{0.95}\text{Mg}_{0.05}\text{O}_2$ thin films; delafossite; low resistivity p-type materials; magnetron system; sputtering current.*

I. INTRODUCTION

ABO_2 (1:1:2) is the general formula of delafossite material, where A is monovalent metals (i.e. the oxidation number is +1, including Pt, Pd, Ag or Cu) and B is trivalent metallic elements (i.e. the oxidation number is +3, including Cr, Fe, Ga, In or Al) [1]. In the delafossite structure, A atom directly bonds in a straight line with 2 oxygen atoms and forms a plane layer, while B atom is surrounded by six oxygen atoms which forms octahedral structure BO_6 . Especially, delafossite has a layer structure with an alternation of A atom plane and BO_6 layer like the structure of NaCoO_2 and $\text{Ca}_3\text{Co}_4\text{O}_9$ materials which are good thermoelectric materials [2, 3]. In the family of delafossite materials, CuCrO_2 emerges as a potential candidate because it has high conductivity in both forms of thin films and bulks. R. Nagarajan had fabricated a 5% Mg-doped CuCrO_2 film with record high conductivity of 220 S/cm [4] unbroken for a long time. However, in 2018, this record was surpassed by result of M. Ahmadi et al. who fabricated a Mg and N co-doped CuCrO_2 thin film obtained a high conductivity value of 278 S/cm [5]. CuCrO_2 delafossite material is an inherent p-type

semiconductor used in many applications such as photo-electronics [6, 7], catalysis [8, 9], thermoelectricity [10, 11], sensor [12], or perovskite solar cell [13]. However, the performance of this material and other p-type materials needs to significantly improve to employ in those applications. For thin film delafossite materials fabricated by the sputtering method, the electrical conductivity of the films is strongly affected by the sputtering conditions: substrate temperature, film thickness, sputtering gas, sputtering currents... Therefore, in this study, we investigate the influence of sputtering currents on the structure, optical properties, electrical properties of 5 %at. Mg-doped CuCrO_2 thin films which fabricated by magnetron sputtering with the change of the sputtering current.

II. EXPERIMENTAL DETAILS

Synthesis

$\text{CuCr}_{0.95}\text{Mg}_{0.05}\text{O}_2$ target is made up from raw oxides of Cu_2O , Cr_2O_3 , MgO (the purity > 99% for all). The powders of those oxides are weighed and then mixed with distilled water. The mixture is put in a mill made of Al_2O_3 and grinded for 5 hours by a planetary ball mill. After the grinding process, the wet mixture is dried out water and pressed into form of a disk. After being pressed, the target was calcined at 1400 °C in a furnace. The Table 1 depicts the detailed conditions for the sputtering process of the thin films.

Table 1. Parameters for the deposition process of $\text{CuCr}_{0.95}\text{Mg}_{0.05}\text{O}_2$ thin films.

Parameters	Details
Target material	$\text{CuCr}_{0.95}\text{Mg}_{0.05}\text{O}_2$
Substrate	soda-lime glass
Sputtering currents	200 - 450 mA
Sputtering gas	Argon
Working pressure	3×10^{-3} torr
Distance between the target and substrate (cm)	5
Temperature of substrate	450 °C

Characterizations

The Bruker D-8 Advanced system was used to investigate the crystal structure of films and measures in 2θ scan = 30–70° (step = 0.02°). The transmittance spectra measured in a wavelength range of 340–1100 nm was carried out by using Jasco V-530 system. The Hall measurement (Ecopia HMS-3000 system) based on Van der Paw method was used to measure carrier concentration and resistivity of the films at room temperature. The surface and cross-section morphology of the films were imaged by Hitachi S-4800 system.

III. RESULTS AND DISCUSSIONS

The diagrams of X-ray diffraction of thin films $\text{CuCr}_{0.95}\text{Mg}_{0.05}\text{O}_2$ deposited under different sputtering currents in Fig. 1 shows that all samples have delafossite structure according to PDF file # 74-0983 standard. The two diffraction peaks (012) and (110) of the delafossite phase exist at the positions of $2\theta = 36.4^\circ$ and 62.5° for all films, respectively. Besides, based on the deconvoluted patterns in Fig. 1b, there is also existent (002) peak at

ca. 35.6° belonged to CuO phase (PDF # 45-0937) and this peak is overlapped with (012) peak of delafossite phase. It is interesting that when the sputtering current increases, the intensity of the diffraction peak (110) of the delafossite phase also grows accordingly. Specifically, when the sputtering current increases from 200 to 350 mA, diffraction peak intensity (110) also increases and reaches a maximum value at the sputtering current of 350 mA. However, the intensity of this peak (110) decreases as the sputtering current increases to 400 mA. In this work, crystal structure of films shows the preferred orientation following the (110) peaks, whereas in other literatures the orientation of XRD peaks only grows in (006) or (012) peaks [14-16].

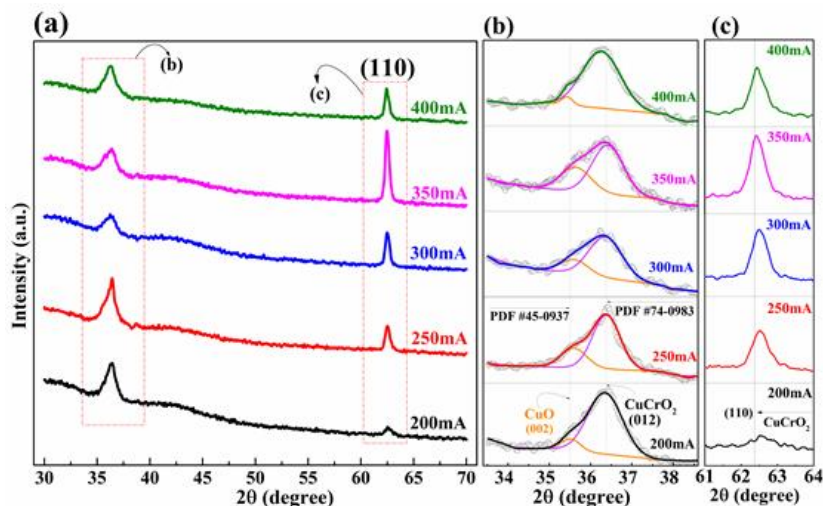


Fig. 1. a) XRD patterns of $\text{CuCr}_{0.95}\text{Mg}_{0.05}\text{O}_2$ thin films at different sputtering currents. b) and (c) are the small 2-theta range of $34 - 38^\circ$ and $61 - 64^\circ$, respectively. Besides, the 2-theta range in (b) was deconvoluted to detect the existence of phases in the films using Pearson VII function for fitting.

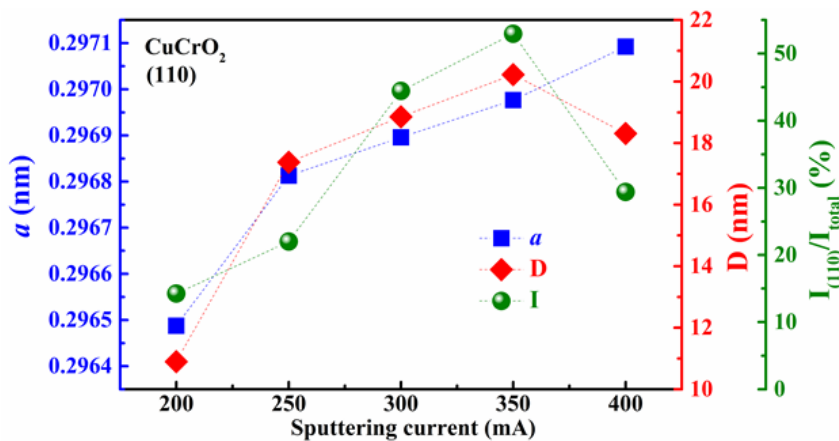


Fig. 2. The dependance of lattice parameter a (nm), the crystallite size D (nm) and the ratio of integrated intensity of diffraction peak (110) and the total integrated intensity of full XRD pattern as a function of sputtering currents.

The change of lattice parameter a , crystallite size D obtained from peak (110), and ratio of integrated intensity of peak (110) and total integrated intensity of full XRD pattern are shown in Fig. 2 as a function of sputtering currents. As seen in Fig. 2, the lattice parameter a increases as sputtering currents increase. This could be explained by the

substitution of the Mg^{2+} ion for the Cr^{3+} ions, because the radius of Mg^{2+} ions (0.72 Å) is larger than Cr^{3+} (0.615 Å) [17]. Therefore, the substitution of Mg^{2+} ions for Cr^{3+} ions given rise to the broaden of lattice parameter a is proportional to the sputtering current. In addition, when the sputtering current increases from 200 to 350 mA, both the crystallite size and the $I_{(110)}/I_{total}$ ratio increase and then there is a slight decrease of those values as the sputtering current increases up to 400 mA. At the sputtering current of 350 mA, the crystal size reached a maximum value of 20.22 nm. From XRD results, it can be clearly seen that the sample prepared at the sputtering current of 350 mA has the optimal crystallinity which is expected to a good electrical conductivity.

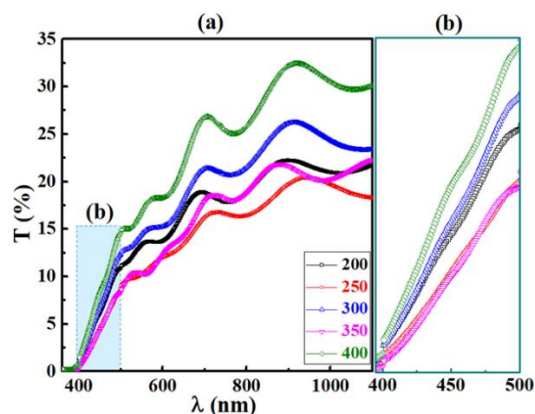


Fig. 3. The transmittance spectra of $CuCr_{0.95}Mg_{0.05}O_2$ thin films at various sputtering currents.

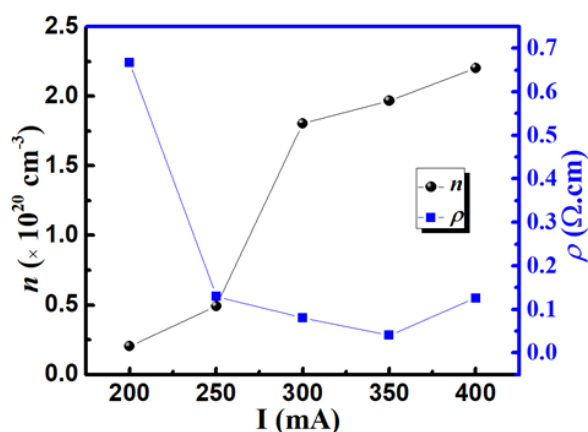


Fig. 4. The hole concentration (n) and resistivity (ρ) of $CuCr_{0.95}Mg_{0.05}O_2$ thin films as a function of sputtering currents.

Fig. 3 shows the transmittance spectra of thin films $CuCr_{0.95}Mg_{0.05}O_2$ deposited at different sputtering currents. In the wavelength range of 400 to 500 nm, the transmittance is relatively low, only 15% or less. The transmittance has an increase with the increase of the sputtering current which implies the improvement of the crystallinity of the films.

The carrier concentration (n) and resistivity (ρ) values of thin films show a significant change with the increase of the sputtering current as shown in Fig. 4. The carrier concentration of sample prepared at 200 mA has the lowest value of $0.2 \times 10^{20} \text{ cm}^{-3}$ while that of 400 mA film reaches the highest value of $2.2 \times 10^{20} \text{ cm}^{-3}$. The carrier concentration and resistivity are two inverse quantities related to each other through the expression: $1/\rho = n \cdot \mu \cdot h$, where μ is the hole mobility and h is the elemental charge ($1.6 \times 10^{-19} \text{ C}$). Therefore, as the carrier concentration increases, the resistivity of the material decreases. The film prepared at the sputtering current of 350 mA achieved the lowest resistivity value is $4 \times 10^{-2} \text{ } \Omega \cdot \text{cm}$. This resistivity value is lower than that of other literatures prepared in similar method [18, 19].

The surface and cross-section morphology of the films shown in Fig. 5 contribute to the explanation of the resistivity values of the sample deposited with a sputtering current of 350 mA. The film surface deposited at sputtering current of 350 mA exhibits a smooth surface in comparison with that of 200 mA as seen in FESEM and cross-section images. Besides, the surface of 350 mA-film appears the grains which may be the crystallite grains of the films. In addition, cross-section images also showed that the structure of the 350 mA-

films has a crystal structure, while this cannot be seen at 200-mA films. From FESEM images, it can be clearly seen that the sputtering current strongly effects on the crystal structure of the films.

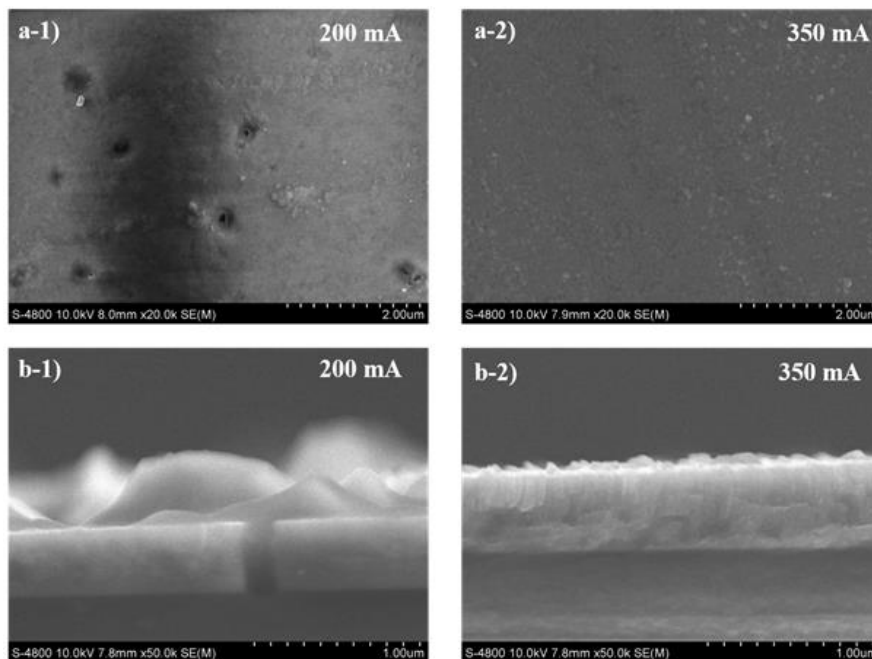


Figure 5: a-1, a-2) Surface FESEM and b-1, b-2) Cross section FESEM of the film deposited at current of 200 mA and 350 mA.

IV. CONCLUSION

In this study, we have systematically studied the effects of the sputtering currents on the structure, optical and electrical properties of thin film $\text{CuCr}_{0.95}\text{Mg}_{0.05}\text{O}_2$ deposited by magnetron sputtering. The results showed that delafossite structure is easy to form regardless the sputtering currents which is different from other literatures. All films exhibit the low transmittance, and the increase of sputtering current gives rise to the increase of the transmittance which implies the improvement of the crystal structure. An increase of the sputtering current leads to an increase in the carrier concentration and a decrease in resistivity. With the sputtering current value of 350 mA, the film has a flat surface, high uniformity of the structure and the lowest resistivity value of $4 \times 10^{-2} \Omega \cdot \text{cm}$ which is relatively low in comparison with other literatures.

ACKNOWLEDGMENTS. This work was supported by the Vietnam Ministry of Science and Technology under grant number ĐTĐL.CN-23/18.

REFERENCES

- [1] M. A. Marquardt, N. A. Ashmore, and D. P. Cann, Crystal chemistry and electrical properties of the delafossite structure, *Thin Solid Films*, **496**(1), 2006, 146-156.
- [2] M. Ohtaki, Oxide Thermoelectric Materials for Heat-to-Electricity Direct Energy Conversion, *Kyushu Univ. Glob. COE Progr. Nov. Carbon Resour. Sci. Newsl.*, **3**, 2010, pp. 8.

- [3] P. Brinks and M. Huijben, *Thermoelectric oxides*. Elsevier Ltd, 2015.
- [4] R. Nagarajan, A. D. Draeseke, A. W. Sleight, and J. Tate, p-type conductivity in $\text{CuCr}_{1-x}\text{Mg}_x\text{O}_2$ films and powders, *J. Appl. Phys.*, **89**(12), 2001, pp. 8022-8025.
- [5] M. Ahmadi, M. Asemi, M. Ghanaatshoar, M. Ahmadi, M. Asemi, and M. Ghanaatshoar, "Mg and N co-doped CuCrO_2 : A record breaking p-type TCO," *Appl. Phys. Lett.*, **242101**(113), 2018, pp. 5051730.
- [6] A. Barnabé, E. Mugnier, L. Presmanes, and P. Tailhades, Preparation of delafossite CuFeO_2 thin films by rf-sputtering on conventional glass substrate, *Mater. Lett.*, **60**(29-30), 2006, pp. 3468-3470.
- [7] X. Li, Temperature-dependent band gap, interband transitions, and exciton formation in transparent p-type delafossite $\text{CuCr}_{1-x}\text{Mg}_x\text{O}_2$ films, **035308**, 2014, pp. 1-8.
- [8] R. Rao, A. Dandekar, R. T. K. Baker, and M. A. Vannice, Properties of Copper Chromite Catalysts in Hydrogenation Reactions, *Journal of Catalysis*, **419**, 1997, pp. 406-419.
- [9] A. P. Amrute, Z. Łodziana, C. Mondelli, F. Krumeich, and J. Pérez-Ramírez, Solid-State Chemistry of Cuprous Delafossites: Synthesis and Stability Aspects, *Chem. Mater.*, **25**(21), 2013, pp. 4423-4435.
- [10] I. Sinnarasa and Y. Thimont, Thermoelectric and Transport Properties of Delafossite CuCrO_2 :Mg Thin Films Prepared by RF Magnetron Sputtering, *Nanomaterials*, **7**(7), 2017, 157.
- [11] R. Manickam and K. Biswas, Double doping induced power factor enhancement in CuCrO_2 for high temperature thermoelectric application, *J. Alloys Compd.*, **775**, 2019, pp. 1052-1056.
- [12] S. Zhou *et al.*, Chemical Room temperature ozone sensing properties of p-type CuCrO_2 nanocrystals, *Sensors and Actuators B*, **143**, 2009, pp. 119-223
- [13] W. A. Dunlap-Shohl *et al.*, Room-temperature fabrication of a delafossite CuCrO_2 hole transport layer for perovskite solar cells, *J. Mater. Chem. A*, **6**(2), 2018, pp. 469-477.
- [14] T. S. Tripathi and M. Karppinen, Enhanced p-Type Transparent Semiconducting Characteristics for ALD-Grown Mg-Substituted CuCrO_2 Thin Films, *Adv. Electron. Mater.*, **3**(6), 2017, 1-7.
- [15] R. Bywalez, S. Götzendörfer, and P. Löbmann, Structural and physical effects of Mg-doping on p-type CuCrO_2 and $\text{CuAl}_{0.5}\text{Cr}_{0.5}\text{O}_2$ thin films, *J. Mater. Chem.*, **20**(31), 2010, pp. 6562-6570.
- [16] M. Ahmadi, M. Asemi, and M. Ghanaatshoar, Mg and N co-doped CuCrO_2 : A record breaking p-type TCO, *Appl. Phys. Lett.*, **113**(24), 2018, pp. 242101.
- [17] I. C. Kaya, M. A. Sevindik, and H. Akyıldız, Characteristics of Fe- and Mg-doped CuCrO_2 nanocrystals prepared by hydrothermal synthesis, *J. Mater. Sci. Mater. Electron.*, **27**, 2015, pp. 1-8.
- [18] I. Sinnarasa, Y. Thimont, L. Presmanes, C. Bonningue, A. Barnabé, and P. Tailhades, Influence of thickness and microstructure on thermoelectric properties of Mg-doped CuCrO_2 delafossite thin films deposited by RF-magnetron sputtering, *Appl. Surf. Sci.*, **455**, 2018, pp. 244-250.
- [19] H. Sun, M. Arab Pour Yazdi, F. Sanchette, and A. Billard, Optoelectronic properties of delafossite structure $\text{CuCr}_{0.93}\text{Mg}_{0.07}\text{O}_2$ sputter deposited coatings, *J. Phys. D: Appl. Phys.*, **49**(18), 2016, 185105.